Synthesis of tuneable amphiphilic-modified polyketone polymers, their complexes with 5,10,15,20-tetrakis-(4-sulfonatophenyl)porphyrin, and their role in the photooxidation of 1,3,5-triphenylformazan confined in polymeric nanoparticles

Araya-Hermosilla, Esteban; Abbing, Marnix Roscam; Catalan-Toledo, Jose; Oyarzun-Ampuero, Felipe; Pucci, Andrea; Raffa, Patricio; Picchioni, Francesco; Moreno-Villoslada, Ignacio

Published in:
Polymer

DOI:
10.1016/j.polymer.2019.01.079

Polymer 167 (2019) 215–223

Contents lists available at ScienceDirect

Polymer

journal homepage: www.elsevier.com/locate/polymer

Synthesis of tuneable amphiphilic-modified polyketone polymers, their complexes with 5,10,15,20-tetrakis-(4-sulfonatophenyl)porphyrin, and their role in the photooxidation of 1,3,5-triphenylformazan confined in polymeric nanoparticles

Esteban Araya-Hermosilla[a], Marnix Roscam Abbing[a], José Catalán-Toledo[b], Felipe Oyarzun-Ampuero[c], Andrea Pucci[d], Patricio Raffa[a], Francesco Picchioni[a], Ignacio Moreno-Villoslada[b,*]

[a] Department of Chemical Engineering – Product Technology, University of Groningen, Nijenborgh 4, 9747 AG, Groningen, the Netherlands
[b] Instituto de Ciencias Químicas, Facultad de Ciencias, Universidad Austral de Chile, Casilla 567, Valdivia, Chile
[c] Department of Sciences and Pharmaceutical Technologies, Universidad de Chile, Santiago, Chile
[d] Department of Chemistry and Industrial Chemistry, University of Pisa, Via Moruzzi 13, 56124, Pisa, Italy

HIGHLIGHTS

- Formazan nanoparticles are used as pollutant pigment model in aqueous media.
- 5,10,15,20-Tetrakis-(4-sulfonatophenyl)porphyrin cannot photooxidize the pollutant.
- A water-soluble polymer is tailored with positive charges and high hydrophobia.
- The photosensitizer forms a complex with the polymer avoiding self-aggregation.
- The complex diffuses into the pollutant particle and photooxidation is catalyzed.

ARTICLE INFO

Keywords:
Amphiphilic cationic polymers
5,10,15,20-Tetrakis-(4-sulfonatophenyl) porphyrin (TPPS)
Photocatalysis

ABSTRACT

A series of amphiphilic polymers bearing aliphatic secondary amines and hydroxyl groups have been synthesized showing different hydrophilic/hydrophobic balance. The synthesis is performed through the Paal-Knorr modification of a polyketone comprising both ethylene and propylene comonomers with *N*-(2-hydroxyethyl)ethylenediamine. The values of dicarbonyl conversion achieved were 19, 35, 51, and 63%, which allowed controlling the amphiphilia of the polymers: a lower carbonyl conversion degree implies a higher hydrophobia. On the other hand, photodegradation studies of a model nanosized pollutant pigment comprised of 1,3,5-triphenylformazan nanoparticles stabilized by poly(sodium 4-styrenesulfonate) have been performed in the absence and in the presence of the photocatalyst 5,10,15,20-tetrakis-(4-sulfonatophenyl)porphyrin, showing no catalytic action, since electrostatic repulsion minimize molecular contacts between the reactants. However, the synthesized polymers allow overcoming this problem. Due to their amphiphila, the polymers showing dicarbonyl conversion values of 35, 51, and 63% form complexes with the porphyrin and stabilize its non-self-aggregated tetraanionic form in water from basic pH up to pH 1.74, 1.82, and 2.76, respectively, the differences related with the polymeric relative hydrophilic/hydrophobic balance. Only the amphiphilic polymer showing a conversion degree of 35% acts as an adequate vehicle for the dye to photocatalyze the oxidation of 1,3,5-triphenylformazan confined in the nanoparticles, highlighting the potential of the Paal-Knorr modification of polyketones to achieve a fine tunning of polymeric properties to obtain a specific functionality: the positive charge of the complex and the high hydrophobia of the tuned polymer allow, respectively, attractive long-range electrostatic interactions with the nanoparticles and diffusion of the reactants into the nanoparticle hydrophobic environment.

* Corresponding author.
E-mail addresses: andrea.pucci@unipi.it (A. Pucci), p.raffa@rug.nl (P. Raffa), imorenovilloslada@uach.cl (I. Moreno-Villoslada).

https://doi.org/10.1016/j.polymer.2019.01.079
Received 20 November 2018; Received in revised form 25 January 2019; Accepted 28 January 2019
Available online 29 January 2019
0032-3861/

1. Introduction

Remediation of waste waters by photodegradation of dyes and pigments is an important challenge that, once overcome, may furnish significant environmental benefits [1–5]. Target dye molecules, both hydrophobic and hydrophilic, are often stabilized in water in amphiphilic matrices [6–8]. These matrices may represent a physical barrier for photocatalysts to reach the target molecule and perform their catalytic effect. The adequate selection of the photocatalysts to achieve a good performance towards the degradation of stabilized dyes and pigments in water involves, among other features, that effective molecular proximity occurs, trespassing physical barriers. 5,10,15,20-Tetrakis-(sulfonatophenyl)porphyrin (TPPS) is a meso-substituted water-soluble porphyrin recognized by its photocatalytic properties, acting as photosensitizer. The dye has the tendency to self-aggregate at increasing concentrations, a fact that may jeopardize its photocatalytic action [9]. Typical highly hydrophilic cationic polyelectrolytes such as chitosan or poly(allylamine) (PALA) [10–12] enhance the self-aggregation of the dye on the polymer surface, since charge repulsion between dyes is overcome by charge attraction between dye and polymer. However, aggregation of this photosensitizer may be avoided by complexation with uncharged amphiphilic polymers that strongly interact with the dye by preferential solvation, such as poly(*N*-vinyl pyrrolidone) (PVP) [13,14], or even amphiphilic cationic polymers presenting charged aromatic groups, such as poly(4-vinyl pyridine) (P4VPy) [11,12] or polyketones derivatized with aromatic amines such as histamine [11], since aromatic-aromatic interactions between the dye and the respective polymers are prevalent over the dye self-aggregation, and the dye disperses on the polymer domain. It remains the question whether amphiphilic cationic polymers with the positive charge placed in aliphatic groups are able to disperse the photosensitizer TPPS, as uncharged amphiphilic polymers do, or enhance the dye self-aggregation as aliphatic hydrophilic polycations do.

Water-soluble amphiphilic polyketone dervatives represent an interesting class of polymeric materials for complexation and encapsulation of charged aromatic molecules [11,12,14–17]. Polyketones are alternate copolymers made of an olefin (typically both ethylene and propylene at different relative composition) and carbon monoxide, aiming at the obtainment of a polymer composed of 1,4-diketone segments. These polymers can be easily functionalized by reaction with a primary amine through the Paal-Knorr reaction [11,15,17,18]. This reaction is solvent and catalysts free, carried out in one-pot, and yields water as the only by-product. The number of primary amines that may be used to derivatize polyketones is countless. Aliphatic or aromatic, charged or uncharged hydrophilic residues can be, then, incorporated, giving rise to water-soluble amphiphilic polymers, containing a hydrophobic backbone consisting of unreacted 1,4-dicarbonyl units and N-substituted pyrrol moieties appearing after the Paal-Knorr reaction, and the hydrophilic pendant groups. The hydrophilic/hydrophobic balance of the copolymers may be tuned by changing the degree of dicarbonyl group conversion (x). Thus, the Paal-Knorr reaction on polyketones represents a simple, low cost, and straightforward way to prepare amphiphilic polymers with tuneable hydrophilic/hydrophobic balance [15,16].

Formazan derivatives represent an important family of pigments of different solubility that are widely used as indicators in various biological applications, such as counting bacterial colonies or testing viability of seeds, measuring mitochondrial activity [19]. The water-insoluble 1,3,5-triphenylformazan (TF) is obtained by reduction of the water-soluble precursor 2,3,5-triphenyl-2*H*-tetrazolium chloride (TTC) [15,20–22]. As a means to stabilize the insoluble TF in aqueous media, we have recently reported the formation of TF nanoparticles in water stabilized by aromatic polyelectrolytes [15,20] such as poly(sodium 4-styrenesulfonate) (PSS) [20]. The reported synthesis avoids the use of organic solvents. It is based on the occurrence of short-range aromatic-aromatic interactions between the precursor TTC and the aromatic groups of the aromatic polyelectrolytes, releasing water from their hydration sphere, so that the reduction reaction is held in the polymer domain. These stabilized TF nanoparticles have been included in different devices, such as hydrogels and polysaccharide films, serving as indicators of changes in environmental redox conditions. However, the potential use of pigments stabilized in nanosized matrices may result in environmental problems if the nanometric products pollute water.

In this paper we will show the synthesis of polyketones derivatized through the Paal-Knorr reaction with *N*-(2-hydroxyethyl)ethylenediamine (HEDA), showing different values of x. The resulting derivatized water-soluble polymers present, thus, the positive charge pending on aliphatic groups, and different balance of hydrophilic/hydrophobic moieties. These copolymers will be used to form complexes with TPPS. In addition, TF/PSS nanoparticles will be used as model nanosized pollutant pigment in water, and the TF photodegradation kinetics will be studied in the absence and in the presence of the photocatalyst TPPS and its polyketone complexes. We hypothesize that the amphiphilic cationic polymers synthesized here may act as vehicles of the photosensitizer to locate it near the TF molecules in the TF/PSS nanoparticles, based on the electrostatic interaction between the complementary charged polymers, and the necessary hydrophobic character afforded by the amphiphilic polymers to allow the photosensitizer diffusing near the hydrophobic TF.

2. Experimental

2.1. Reagents

HEDA (Sigma-Aldrich, 99%), 2,5-hexanedione (Sigma-Aldrich, 98%), TPPS (TCI), TTC (Merck, 95%), ascorbic acid (Sharlau, 99.7%) and PSS (Sigma-Aldrich, M_w 70 000 g/mol) were commercially available and used as received. Polyketones made of ethylene, propylene and carbon monoxide were synthesized according to reported procedure [23,24]. In particular, a polyketone comprised of 50% ethylene and 50% propylene (PK50, Mw 3261, PDI 3, calculated by GPC) was used. Distilled water, 1-propanol (Sigma-Aldrich) and $CDCl_3$ (Sigma-Aldrich) were used as solvents. The pH was adjusted with minimum amounts of HCl (Sigma-Aldrich) and NaOH (Sigma-Aldrich). The structures of the molecules and reactions involved are shown in Fig. 1.

2.2. Equipment

Water was deionized in Arium 611 Sartorius deionizer. The polymer synthesis was performed in a microwave CEM Discover. UV–vis measurements were performed in a Cary 100 Bio UV–vis spectrophotometer and a Jasco V-750 UV–vis spectrophotometer equipped with a STR-773 water thermostatted cell holder with stirrer (Jasco), connected to a heating bath circulator RW-2025G (Lab Companion). ^{1}H NMR measurements were made in a Varian Mercury Plus 400 MHz spectrometer. ATR-FT-IR spectra were recorded using a Thermo Nicolet NEXUS 670 FT-IR. Elemental analysis measurements were performed with a Euro EA elemental analyzer. The pH was controlled on a Seven2Go™ pH meter. A 45 W LED lamp panel (Mokoqi) composed of 148 red (650 nm), 36 blue (465 nm), 17 orange (606 nm), and 24 white LED devices was used as a source of light for photooxidation studies.

2.3. Procedures

Model compound synthesis. A model compound was synthesized as a reference for the characterization of the polymers after the Paal-Knorr reaction. The reaction between stoichiometric amounts of HEDA and 2,5-hexadione was performed in a 100 mL round bottom flask equipped with a magnetic stirrer and a reflux condenser. 0.46 g of 2,5-hexadione (0.004 mol) and 0.42 g of HEDA (0.004 mol) were dissolved in 30 mL of 1-propanol and transferred to a microwave oven. The reaction was carried out during 150 min at 100 °C (100 W). In order to fully

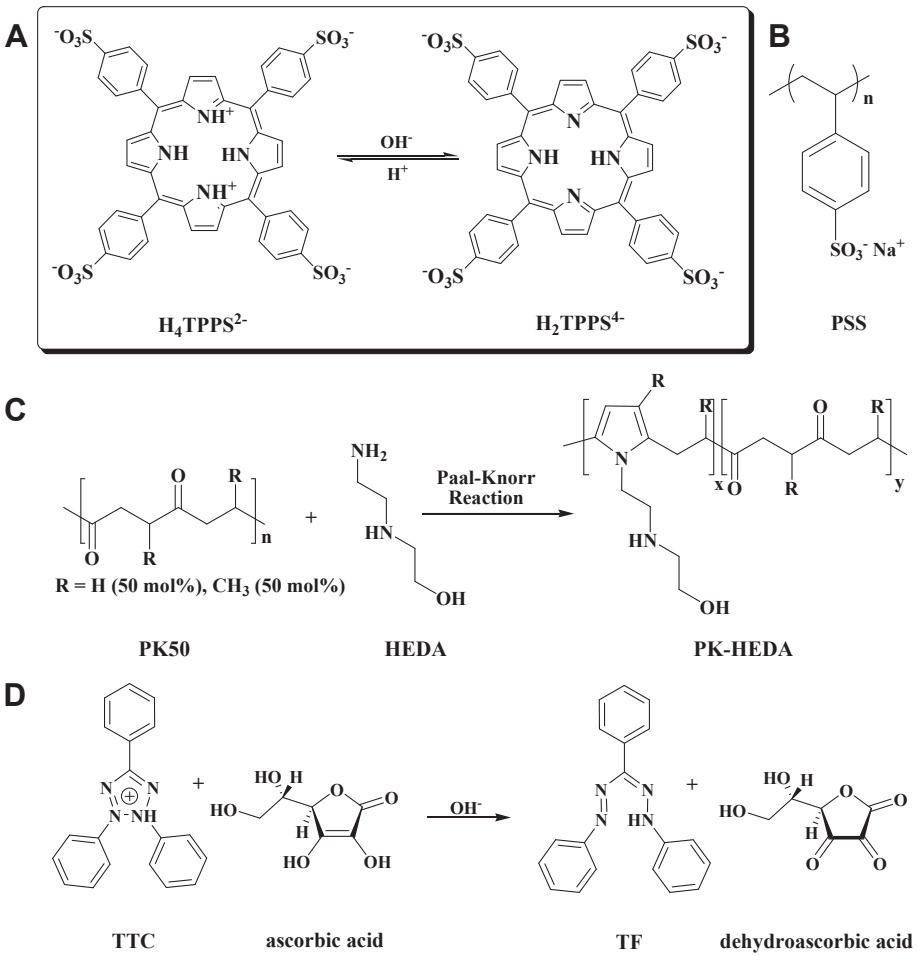

Fig. 1. Molecular structures and reactions: **A**: protonation equilibrium in TPPS; **B**: PSS; **C**: PK50 derivatization with HEDA; **D**: TF formation upon reduction of TTC with ascorbic acid.

Table 1
Amounts in the feed and value of x after Paal-Knorr reaction between PK50 and HEDA.

Polyketone derivative (PK50HEDAx)	PK50 (g)	Moles of di-carbonyl group	HEDA (g)	Moles of HEDA	N (%)	x	M_+ (g/mol of basic groups)
PK50HEDA19	19.65	0.16	3.25	0.031	3.79	0.19	731
PK50HEDA35	19.05	0.15	6.30	0.061	6.54	0.35	428
PK50HEDA51	19.56	0.16	9.70	0.093	8.88	0.51	315
PK50HEDA63	19.24	0.15	12.72	0.122	10.32	0.63	268

evaporate the solvent, the sample was placed in an oven for 48 h at 50 °C. The product was analyzed by ^{1}H NMR in $CDCl_3$. δ = 2.2 ppm (s, 6 H, CH_3), 2.7 ppm (m, 2H, distal aliphatic N−CH_2), 2.9 ppm (t, 2H, proximal aliphatic N−CH_2), 3.6 ppm (m, 2H, O−CH_2), 3.9 ppm (t, 2H, aromatic N−CH_2), 5.8 ppm (s, 2H, =CH−CH =). *Polyketone derivative synthesis.* Functionalization of PK50 with HEDA was carried out similarly. In order to achieve different 1,4-dicarbonyl/primary amine molar ratios, the amount of the primary amine is varied, as listed in Table 1. Thus, around 20 g of PK50 and variable amounts of HEDA were placed in a 100 mL round bottom flask equipped with a magnetic stirrer and a reflux condenser, without using any solvent. The reaction mixture was transferred to the microwave apparatus, and the microwave power was kept at 100 W during 150 min at a temperature of 100 °C. The products were further purified by solvent extraction technique, using brine and chloroform as solvents. Chloroform was evaporated in a vacuum oven at 50 °C and 0 bar for 48 h. The polymers were characterized by ^{1}H NMR in $CDCl_3$ and ATR-FT-IR. The value of x was calculated by elemental analysis by the following formula [11]:

$$x = \frac{NM_c}{nM_N + N(M_c - M_p)} \quad (1)$$

where N is the nitrogen content per g, M_N represents the atomic mass of nitrogen (14 g/mol), n is the number of nitrogen atoms of the converted 1,4-dicarbonyl segment (2 in this case), M_p is the molecular weight of the converted 1,4-dicarbonyl segment (194 g/mol in this case), and M_c is the molecular weight of the non-converted 1,4-dicarbonyl segment of PK50 (126 g/mol). M_p and M_c were calculated taking into account the incorporation of ethylene and propylene in the copolymers at ratio of 1:1. In order to adjust the stoichiometry of charged groups when using the polyketone derivatives, we consider a polymeric molecular weight (Table 1) given in g/mol of basic groups (M_+) following [11]:

$$M_+ = \frac{xM_p + yM_c}{xz} \quad (2)$$

where y is the fraction of non-converted 1,4-dicarbnyl groups, provided that $x + y = 1$, and z is the number of atoms susceptible to protonate in the converted repetitive unit, 1 in this case, provided that the

dicarbonyl moieties are not susceptible to protonate.

Synthesis of TF/PSS nanoparticles. The starting materials (1 mL of 3×10^{-3} M TTC aqueous solution, 1 mL of 3×10^{-2} M PSS solution, 0.5 mL of 1.2×10^{-2} M ascorbic acid solution, and 0.5 mL of 1.0 M NaOH solution) were mixed in a 1 cm path length quartz vessel, placed in the Jasco spectrophotometer with control of temperature set at 25 °C with the aid of the circulating heating bath and left to stir for 15 min, resulting in the formation of TF nanoparticles in accordance with a described procedure [20]. The reaction progress was monitored by UV–vis spectrometry, and was considered successful when the slope of the curve absorbance at 575 nm versus time (s), during the first 120 s fits in the range 0.00620 and 0.00630 s^{-1}. The apparent concentration of TTC and PSS in the feed was 1×10^{-3} and 1×10^{-2} M, respectively. *Complex formation between the PK50HEDA*x *and TPPS.* Complexation of PK50HEDA*x* and TPPS was performed by mixing stock solutions of both interacting species. In order to measure the transition pH between the tetraanionic and the dianionic species of TPPS, the pH was adjusted between 3.4 and 1.1 with minimum amounts of NaOH and HCl, and was allowed equilibrating overnight. Particular conditions are given in the Figure captions. Absorption UV–vis analyses were performed with path lengths ranging between 0.2 and 1 cm. *Decolouration of TF/PSS nanoparticles photocatalyzed by TPPS/PK50HEDA*x *complexes*. In a glass tube, 5 mL of aqueous suspensions containing 0.5 mL of the TF/PSS nanoparticles synthesized above, and 1×10^{-6} M of TPPS, complexed or not with 5×10^{-4} M of PK50HEDA*x*, were prepared. Assuming a total conversion of TTC into TF, the apparent final concentration of TF and PSS in these samples was 1×10^{-4} and 1×10^{-3} M, respectively. The pH was adjusted to 6. The samples were placed at 10 cm distance under the LED lamp showing irradiance of 50 mW/cm^2. Discoloration of TF was monitored through UV–vis spectra analysis every 15 min under constant stirring at a temperature of 25 °C.

3. Results and discussion

3.1. Polyketone modification

As a first approximation, the screening made on the whole range of possible *x*, between 0 and 1, was chosen to be 0, 0.2, 0.4, 0.6, and 0.8, which is the theoretical limit of conversion due to statistical reasons linked to the reaction occurring at adjacent carbonyls. The products of the Paal-Knorr reaction were analyzed by elemental analysis in order to calculate *x*. The result can be seen in Table 1. Conversion was close to quantitative concerning the stoichiometry of the primary amine included in the feed, mainly for the lowest *x* intended. Thus, at molar ratios in the feed of 80, 60, 40, and 20%, the values of *x* achieved were 0.63, 0.51, 0.35, and 0.19, respectively, values that are included in the respective code names of the polymers (PK50HEDA*x*). The successful functionalization of PK50 with HEDA was confirmed by ATR FT-IR and ^{1}H NMR spectroscopies. Fig. 2A shows the ^{1}H NMR spectra of the different PK50HEDA*x*. The polymeric nature of the molecules, together with a statistical distribution of ethylene and propylene monomers in PK50, as well as the statistical distribution of the converted 1,4-dicarbonyl units, are responsible for the appearance of broad peaks. Using the information obtained from the model compound (see experimental section) facilitates the assignment of the signals. PK50HEDA19, 35, 51, and 63 show their pyrrole rings with proton signals between 5.5 and 6.0 ppm corresponding to protons 1 and 2 after Paal-Knorr reaction with the ethylene and propylene 1,4-dicarbonyl segments, respectively. When the Paal-Knorr reaction is produced on the propylene 1,4-dicarbonyl segment a peak appears at around 2.0 ppm corresponding to the methyl groups (proton 3). Methylene protons 4 and 7 can be clearly assigned at 3.8 and 3.6 ppm, respectively, due to their expected chemical shift. On the other hand, methylene protons 5 and 6 can be assigned to the peaks at 2.8 and 2.7 ppm, respectively, that overlap with the peaks of the residual 1,4-dicarbonyl units, a fact that can be corroborated by comparison to the spectrum of the pristine PK50.

Fig. 2B shows the ATR-FT-IR spectra of PK50HEDA*x*. As the conversion increases, the intensity of the carbonyl group (1700 cm^{-1}) decreases, due to the disappearance of the 1,4-dicarbonyl moieties. The intensity of three medium intensity peaks appearing in the range of 1399-1350 cm^{-1}, which may be attributed to the scissoring bending vibration of the CH_2 next to the carbonyl group, and the symmetrical bending vibration of the CH_3, also decreases as *x* increases. In the range of 3700-3000 cm^{-1} a broad peak appears once the Paal-Knorr reaction is achieved, which corresponds to the hydrogen bonding occurring with exchangeable protons in the pendant group. In the range of 1650-1500 cm^{-1} a series of weak peaks does also appear which can be assigned to stretching of C=N and C=C in the pyrrole ring. The asymmetrical and symmetrical stretching bands of aliphatic C–H of PK50 appearing between 2969 and 2873 cm^{-1} broaden as *x* increases, including the corresponding signals of the HEDA pendant group.

As it might be expected, the hydrophilia of these polymers also increases as *x* increases. Thus, both PK50 and PK50HEDA19 are water-insoluble, while PK50HEDA35, PK50HEDA51, and PK50HEDA63 are water-soluble at a polymer concentration of 1×10^{-4} M and pH 7. A balance between the number of hydrophilic and hydrophobic segments in the polymer chains determines the amphiphilia of the copolymers. Protonation of the amino group at pHs below its pK_a increases the hydrophilia of the polymers.

3.2. Complexation between H_2TPPS^{4-} and PK50HEDAx

TPPS presents protonation equilibrium: in a dilute regime, at pH higher than around 5 the molecule is tetraanionic (H_2TPPS^{4-}), whereas at pH lower than around 5, the porphin group double protonates, giving raise to the dianionic species H_4TPPS^{2-}, being the exact transition pH value dependent on the total concentration. The resulting H_4TPPS^{2-} becomes more hydrophilic, since it presents 6 charges, 4 negative

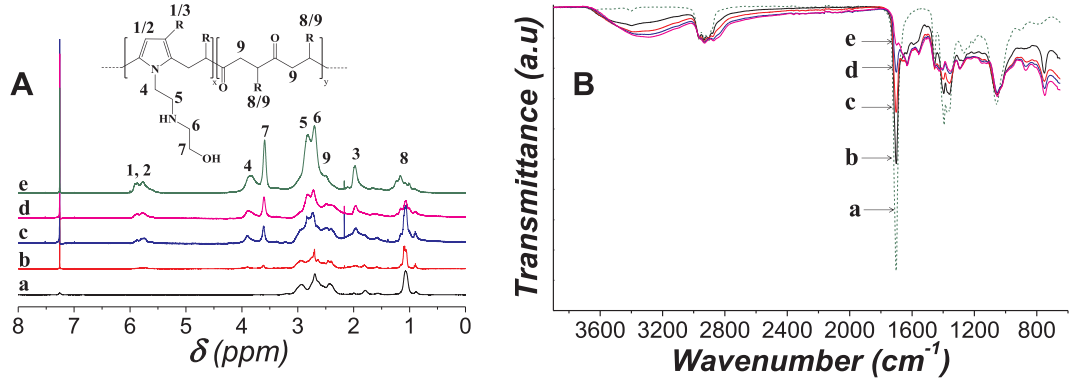

Fig. 2. ^{1}H NMR (**A**) and FT-IR spectra (**B**) of PK50HEDA*x* at values of *x* of: 0.0 (a); 0.19 (b); 0.35 (c); 0.51 (d); 0.63 (e).

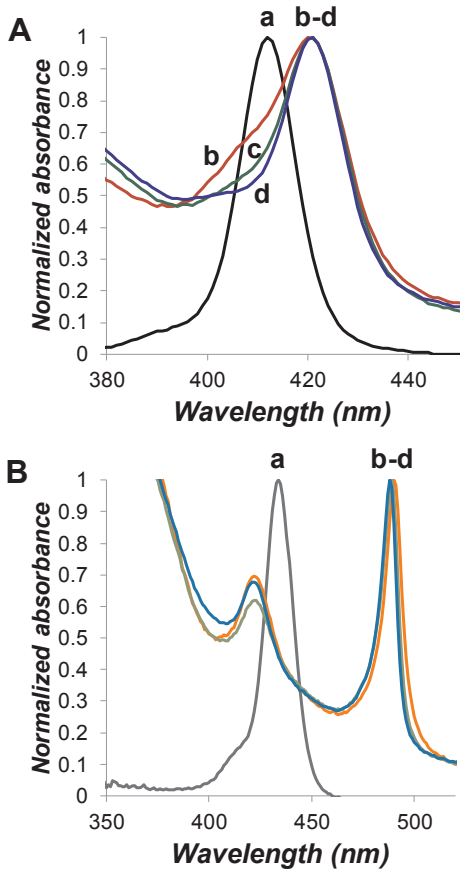

Fig. 3. UV–vis spectra of 10^{-6} M TPPS in the absence (a) and in the presence of 10^{-4} M PK50HEDA63 (b), PK50HEDA51 (c), and PK50HEDA35 (d), at pH over (A) and under (B) the transition pH value between the tetraanionic and the dianionic species.

charges placed at the periphery of the molecule, supported on the phenyl groups, and two positive charges in the center of the molecule. The tetraanionic form presents a maximum at 414 nm in absorbance spectra, as can be seen in Fig. 3, while the dianionic form presents a maximum at 435 nm, corresponding to the Soret band of free, hydrated monomeric species of the dye in both cases. When dilute solutions of H_2TPPS^{4-} are put in contact with 100-fold excess of the different PK50HEDA*x* derivatives, different spectroscopic responses are obtained at different conditions. In the presence of PK50HEDA*x*, the Soret band of the tetraanionic form appears at around 421 nm, indicating total or partial dehydration of the dye due to preferential solvation by the polymer segments through specific interactions. It can be noticed that the less hydrophobic PK50HEDA63 induces partial aggregation of the dye at basic pH as H-aggregates, witnessed by the shoulder at around 400 nm, tending, then, to a behaviour closer to that of hydrophilic aliphatic polycations such as PALA or chitosan. The spectra corresponding to the dianionic form of the dye in the presence of the polymers at pH below the transition pH presents a maximum at around 490 nm, indicating the formation of J-aggregates in water. Indeed, as the dianionic form of the dye is more hydrophilic than the tetraanionic form, it easily detaches from the polymer and hydrates. However, long-range electrostatic interactions produce a concentration gradient of the dye around the polymer chains, so that self-aggregation in the form of head-to-tail aggregates occurs. This interpretation can be contrasted with literature data: in the presence of uncharged amphiphilic polymers such as PVP, the dye is dispersed solvated by the polymer at basic pH, and released from the polymer domain at acid pH, without undergoing self-aggregation due to the lack of electrostatic interactions with the polymer [13]. In the presence of hydrophilic, positively charged

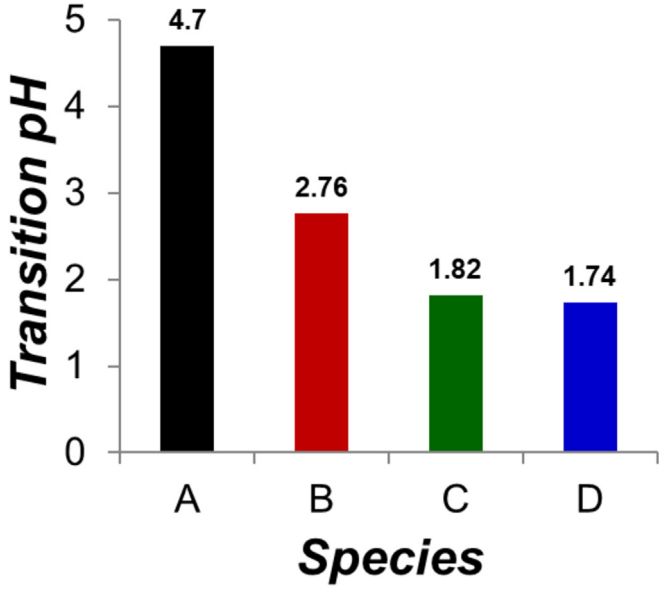

Fig. 4. Transition pH between H_2TPPS^{4-} and H_4TPPS^{2-} for 1×10^{-6} M of the dye in the absence (A) and in the presence of 10^{-4} M of PK50HEDA63 (B), PK50HEDA51 (C), and PK50HEDA35 (D).

polymers such as PALA, the hydrated dye molecules undergo self-aggregation both at pH acid and basic, in the form of J- and H-aggregates, respectively, due to their higher concentration around the polyelectrolyte chains caused by the electrostatic potential furnished by the polymer [11]. Here, we can see that amphiphilic, positively charged polymers, produce interactions with the tetraanionic form of the dye that are able to keep the disaggregated state of the dye through preferential solvation with the polymer segments, and long-range interactions with the dianionic form that produce the porphyrin self-aggregation at acid pH. This offers a pool of technologies to control the state of aggregation of such important dyes for basic research and technological applications.

Pristine TPPS presents a transition pH between its tetra-anionic (H_2TPPS^{4-}) and the di-anionic forms (H_4TPPS^{2-}) of 4.7 at a concentration of 1×10^{-6} M, as can be seen in Fig. 4. The free energy compensation upon preferential solvation produces a stabilization of the tetraanionic form of TPPS at acid pH. Thus, the transition pH between the dianionic and the tetraanionic forms is shifted to lower values in the presence of the different PK50HEDA*x* derivatives, as can be also seen in Fig. 4. The transition pH decreases as *x* decreases, related to the increase on the hydrophobic character of the polymer, since as *x* decreases, the fraction of hydrophobic segments increases with respect to the hydrophilic ones. Thus, the transition pH found for PK50HEDA35, 51, and 63 were 1.74, 1.82, 2.76, respectively. Contrasting with the literature, we can see that amphiphilic polyeketone derivatives presenting cationic aromatic pendant groups, such as imidazolium groups, are able to stabilize the tetraanionic form of the dye to pH lower than 1.5, due to the occurrence of aromatic-aromatic interactions between the dye and the cationic aromatic polymeric residue [11]. Typical polycations do also induce a change on the transition pH to values over 2 at similar conditions, due to that the tetraanionic form is stabilized by the polymeric charge [11]. Uncharged amphiphilic polymers such as PVP stabilize the tetraanionic form of the dye up to pH over 3 at very high excess of the polymer [13], revealing a weaker stabilization effect through preferential solvation.

3.3. Photooxidation of TF/PSS nanoparticles by H_2TPPS^{4-} complexed with PK50HEDAx

Oxidation reactions can be photocatalyzed with the photosensitizer

Table 2
Hydrodynamic diameter, PDI, and zeta potential of TF/PSS nanoparticles pristine and in the presence of TPPS complexed or not with the different PK50HEDA*x* before irradiation.

Sample	Apparent concentration (M)	Hydrodynamic diameter (nm)	PDI	Zeta potential (mV)
TF/PSS	$10^{-4}/10^{-3}$	299	0.151	−64
TF/PSS + TPPS	$10^{-4}/10^{-3} + 10^{-6}$	331	0.207	−56
TF/PSS + TPPS/PK50HEDA35	$10^{-4}/10^{-3} + 10^{-6}/5 \times 10^{-4}$	352	0.297	−47
TF/PSS + TPPS/PK50HEDA51	$10^{-4}/10^{-3} + 10^{-6}/5 \times 10^{-4}$	314	0.228	−49
TF/PSS + TPPS/PK50HEDA63	$10^{-4}/10^{-3} + 10^{-6}/5 \times 10^{-4}$	315	0.208	−49

TPPS, which normally acts through a Type II mechanism by which the energy absorbed from light by the photosensitizer is transferred to oxygen, producing singlet oxygen as an active oxidant [25]. The short lifetime of singlet oxygen in aqueous media reduces the probability of molecular collisions [26]. Thus, a close contact between the photosensitizer and the molecule to be oxidized is desirable. Our target molecule is, in this case, the red coloured TF, which, according to our previous works, can be dispersed in water in the form of nanoparticles stabilized by the negatively charged aromatic polyelectrolyte PSS [20]. However, the polymer itself may act as a steric and electrostatic barrier for the negatively charged TPPS to reach the TF molecules. These energetic barriers may be trespassed if the photosensitizer is adequately vehiculized in cationic, amphiphilic complexes able to undergo electrostatic attraction with the target particle, and allow molecular diffusion of the reactants.

TF/PSS nanoparticles were easily and successfully formed according to the literature [20]. DLS analyses show hydrodynamic diameter of almost 300 nm with low PDI, indicating a narrow distribution of monomodal nanoparticles (see Table 2 and Fig. 5). These nanoparticles show zeta potential of −64 mV, high enough in absolute value to ensure the stability of the nanoparticles in water avoiding their aggregation, thus providing a homogenous suspension of TF in water. Before irradiation, these magnitudes do not change much when the nanoparticles are put in contact with the photosensitizer, both complexed and non-complexed with the different PK50HEDA*x*, as can be read in Table 2. The corresponding STEM images are shown in Fig. 5, where similar nanoparticles of around 300 nm of diameter are clearly observed for all the formulations. It can be noted, however, that the zeta potential of the nanoparticles decreases from −64 to around −48 mV in the presence of the TPPS/PK50HEDA*x* complexes. This is indicating that the positively charged complexes interact with the nanoparticles by electrostatic interactions. The small increase on the size of the nanoparticles may be related to a lower concentration of the complexes and to a balance between shrinking by electrostatic neutralization of

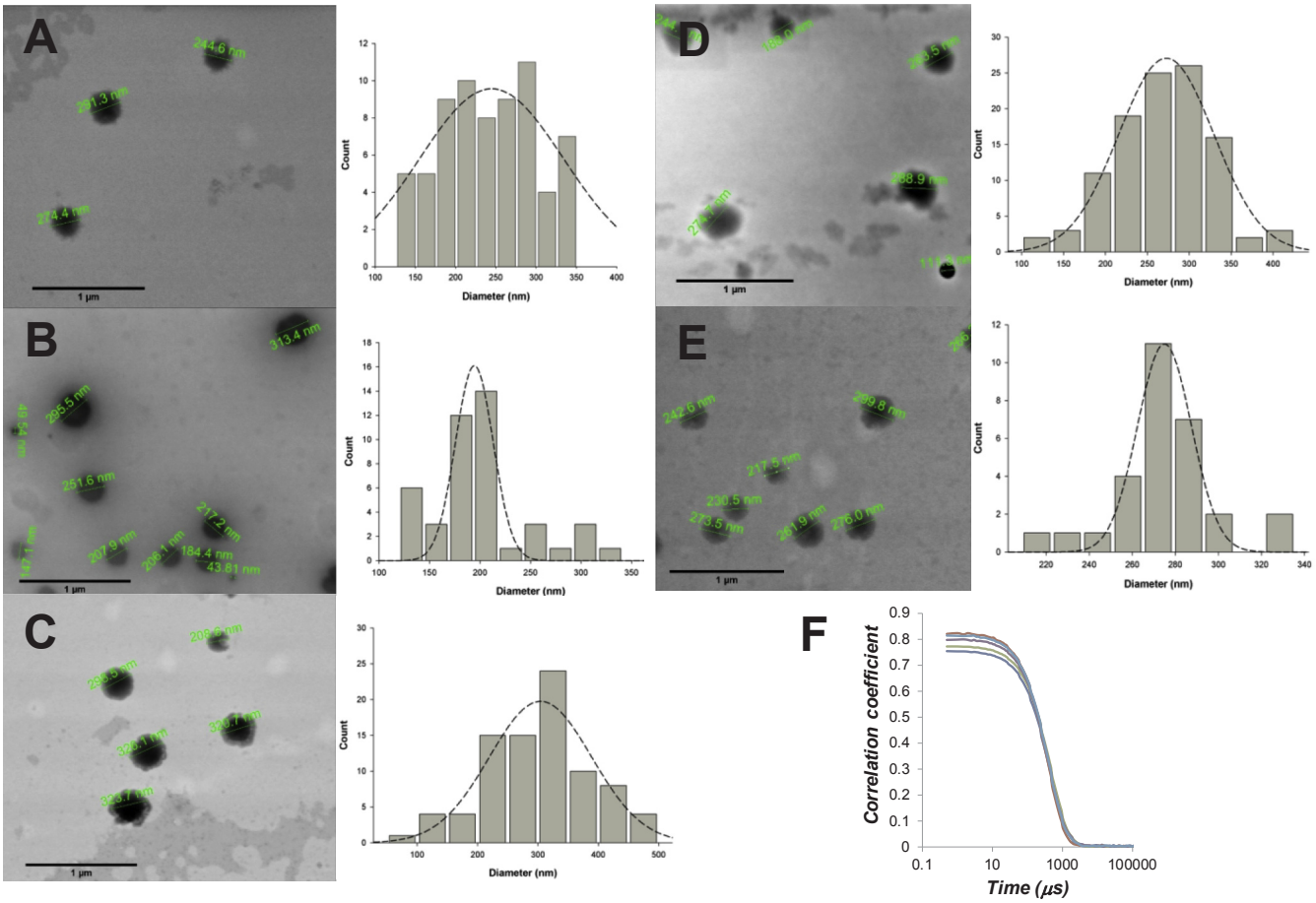

Fig. 5. STEM images and diameter distribution histograms of nanoparticles obtained in suspensions of TF/PSS nanoparticles (1×10^{-4} M/1×10^{-3} M) (A), and the same nanoparticles in the presence of 1×10^{-6} M of H_2TPPS^{4-} (B) and in the presence the respective dye complexes with 5×10^{-4} M of PK50HEDA35 (C), PK50HEDA51 (D), and PK50HEDA63 (E). Scale bar indicates 1 µm. Correlograms corresponding to aqueous suspensions of the formulations (see Table 2) (F).

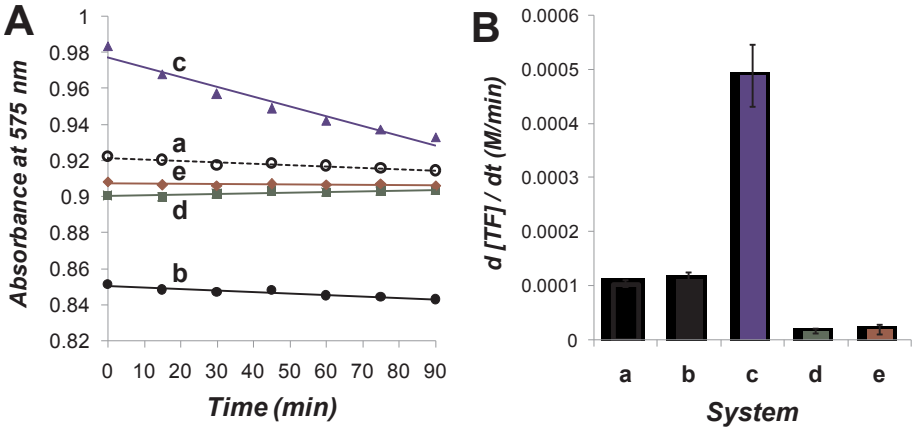

Fig. 6. A: Decay in the absorbance of TF/PSS nanoparticles with time under UV–vis radiation at pH 6 alone (**a**,○), and in the presence of 1×10^{-6} M of TPPS, pristine (**b**,●) and complexed with 1×10^{-4} M of PK50HEDA35 (**c**,▲); PK50HEDA51 (**d**,■); and PK50HEDA63 (**e**,◆). **B**: slopes of the corresponding linear adjustments (n = 3).

the hydrated surface of the nanoparticles and increase on the size by the increase of the total matter of the nanoparticle. The most significant changes in size, PDI, and zeta potential occur in the presence of TPPS/PK50HEDA35, *i. e.*, when the photosensitizer is complexed with the most hydrophobic polymer. In this case, the mass of the hydrophobic residues is higher than in the case of PK50HEDA51 and 63, and polymeric molecular motions may produce swelling if these hydrophobic segments penetrate the nanoparticle.

As can be seen in Fig. 6, irradiation of the TF/PSS nanoparticles induces the spontaneous degradation of the formazan at a slow rate (around 10^{-4} M/min). In the presence of 10^{-6} M of the pristine TPPS, the rate of degradation does not change, as expected, due to that the approximation of the photosensitizer is inhibited by charge repulsion, thus the catalytic photooxidation reaction is minimized. When the dye is complexed with the more hydrophilic PK50HEDA63 and 51 the rate of decolouration decreases. This is consistent with TPPS/PK50HEDA complexes interacting with the negatively charged nanoparticles, without intimately mixing each other. PK50HEDA*x* may furnish opacity to the nanoparticles, since they show a broad band from UV to around 550 nm in the visible region (see baseline in Fig. 3). However, the more hydrophobic PK50HEDA35 produced an increase on the rate of TF degradation with light to almost 5×10^{-4} M/min. Our interpretation is that, due to the higher fraction of hydrophobic segments, once the TPPS/PK50HEDA35 complex interacts electrostatically with the TF/PSS nanoparticles, both species fuse providing a hydrophobic core in which TF and TPPS may diffuse close to each other.

3.4. Final remarks

In this work we have highlighted important concepts regarding i) the synthesis of tuneable amphiphilic polyektone derivatives, ii) the interactions between polymers and dyes in water, and iii) the use of these interactions to produce complexes able to enhance the photocatalytic activity of photosensitizers.

Regarding the first concept, we can consider the functionalization of polyketones via the Paal-Knorr reaction as a simple and cheap method to produce polymers with special properties that can be easily tuned to achieve high specific performances. This is what we can call fine tuning of the polymeric properties, related to the synthetic method and the resulting polymer composition.

Regarding the second concept, we can depict a complete picture concerning the interactions of TPPS at dilute conditions and water-soluble polymers in excess with specific characteristics of aromaticity, charge, amphiphilia, and flexibility. The picture can be schematized as seen in Fig. 7. Uncharged amphiphilic water-soluble polymers solvate the dye at pH above the transition pH between the tetraanionic and the dianionic forms, and desolvate it at pH under the transition pH; this transition pH undergoes a moderate shift to acid values [13]. Typical hydrophilic polycations induce the dye self-aggregation at pH both above and under the transition pH, in the form of H- and J-aggregates, respectively, due to an increase on the local concentration of the dye around the polymer as a consequence of electrostatic interactions; the transition pH undergoes a moderate shift to acid values [11]. Rigid aromatic polycations disperse the dye on their environment, due to the occurrence of aromatic-aromatic interactions at pH above the transition pH, and induce desolvation and J-aggregation at pH under the transition pH; the transition pH undergoes a very high shift to acid values, so that desolvation and J-aggregation may occur at pH below 1.5 [11]. More flexible aromatic polycations such as poly(decyl viologen) (PV10) induce H-aggregation and J-aggregation at both acid and basic pH, showing a very high shift of the transition pH to acid values [11,27]; the H-aggregates of the tetraanionic form of the dye are assumed to be confined in the polymer domain. Amphiphilc aliphatic polycations solvate the dye at pH above the transition pH and induce desolvation and J-aggregation at pH under the transition pH; the transition pH undergoes a high shift to acid values (this paper).

Regarding the third concept, we find in the amphiphilic aliphatic charged polymer PK50HEDA35 an adequate vehicle to enhance the photocatalytic properties of TPPS towards the photooxidation of TF in water, when the formazan is dispersed as nanoparticles stabilized by the aromatic polyelectrolyte PSS. As depicted in Fig. 8, the positive charge of the PK50HEDA35/TPPS complex allows the complex interacting with the negatively charged TF nanoparticle, primary through long-range electrostatic interactions, and then through hydrophobic and/or other secondary interactions. The high hydrophobic character of the polyketone derivative allows, then, molecular rearrangement so that the hydrophobic parts of the complex can diffuse inside the nanoparticle, which may include ion pairs formed between the polymer and TPPS. Thus, intimate contacts between the photocatalyst TPPS and the hydrophobic pigment TF can be produced, overcoming the electrostatic barrier that the negative charge of PSS originates. This phenomenon does not occur with the other synthetic polymers of the series studied here, which gives account of the high specificity of the functionality obtained by PK50HEDA35, very sensitive to the hydrophilic/hydrophobic balance, achieved thanks to the fine tuning possibilities associated to the functionalization of polyketones via the Paal-Knorr reaction.

The findings shown here open new possibilities of applications of dyes and polymers through the interplay of different variables that allow controlling the state of aggregation of the dyes, and phase transitions and migrations at a nanometric scale, which may include catalysis for water remediation or photodynamic therapy.

4. Conclusions

The series of amphiphilic polymers PK50HEDA19, 35, 51 and 63 has been successfully obtained through the Paal-Knorr modification of a polyketone with N-(2-hydroxyethyl)ethylenediamine. The copolymers

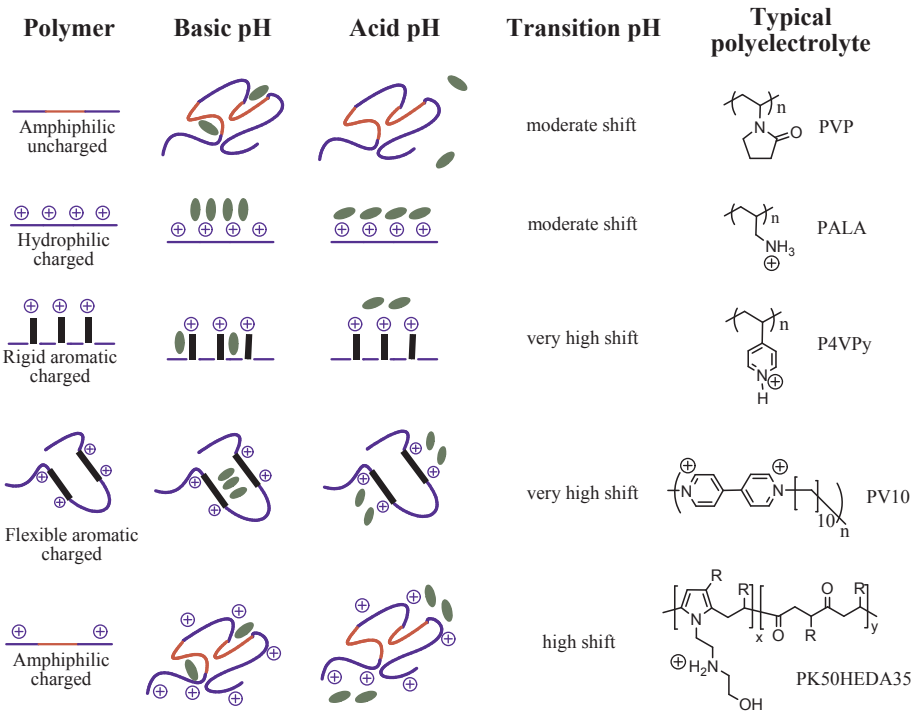

Fig. 7. Scheme depicting the interaction in water between dilute TPPS (⬬) and water-soluble polymers in excess above and under the transition pH values between the tetraanionic and the dianionic form of the dye.

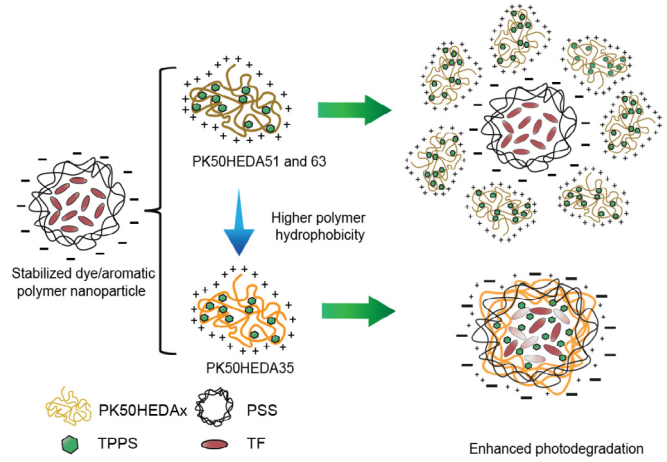

Fig. 8. Scheme depicting the interaction in water between TF/PSS nanoparticles and PK50HEDA35/TPPS complex. After molecular rearrangement, the photocatalyst TPPS (⬢) easily approach the hydrophobic TF molecules (⬬).

bearing secondary amines and hydroxyl groups show different hydrophilic/hydrophobic balance, being the most hydrophobic the one presenting the lowest dicarbonyl conversion degree. PK50HEDA35, 51, and 63 form complexes with TPPS that induce stabilization of the non-self-aggregated tetra-anionic form of the dye in water at a concentration of 10^{-6} M from basic pH up to pH 1.74, 1.82, and 2.76, respectively, while for the pristine dye the transition between its tetraanionic and dianionic forms occurs at pH 4.7. On the other hand, photodegradation of TF/PSS nanoparticles showing negative zeta potential, used as model nanosized pollutant pigment, spontaneously occurs at a rate of 1×10^{-4} M/min. Due to electrostatic repulsion, the presence of TPPS does not enhance the photodegradation of the pigment. Complexes of the photosensitizer with PK50HEDA51 and 63 decrease the rate of photodegradation. However, the more hydrophobic PK50HEDA35/TPPS complex could enhance photodegradation, acting as an adequate vehicle for the dye to photocatalyze the oxidation of the formazan confined in the nanoparticles, allowing diffusion of the reactants in a hydrophobic environment, and achieving a photodegradation rate of 5×10^{-4} M/min.

Acknowledgements

Fondecyt Regular (Chile, Grants No. 1161450, and 1181695), and Fondequip (Chile, Grant No. EQM160157). Esteban Araya-Hermosilla thanks CONICYT, Chile, for Doctoral Fellowship No. 72130047.

References

[1] A. Tehrani-Bagha, K. Holmberg, Solubilization of hydrophobic dyes in surfactant solutions, Materials 6 (2) (2013) 580.
[2] M.A. Rauf, S.S. Ashraf, Fundamental principles and application of heterogeneous photocatalytic degradation of dyes in solution, Chem. Eng. J. 151 (1) (2009) 10–18.
[3] R.J. Tayade, P.K. Surolia, R.G. Kulkarni, R.V. Jasra, Photocatalytic degradation of dyes and organic contaminants in water using nanocrystalline anatase and rutile TiO2, Sci. Technol. Adv. Mater. 8 (6) (2007) 455–462.
[4] S.K. Ling, S. Wang, Y. Peng, Oxidative degradation of dyes in water using Co2+/H2O2 and Co2+/peroxymonosulfate, J. Hazard Mater. 178 (1) (2010) 385–389.
[5] M. Vautier, C. Guillard, J.-M. Herrmann, Photocatalytic degradation of dyes in water: case study of indigo and of indigo carmine, J. Catal. 201 (1) (2001) 46–59.
[6] U. Bazylińska, A. Lewińska, Ł. Lamch, K.A. Wilk, Polymeric nanocapsules and nanospheres for encapsulation and long sustained release of hydrophobic cyanine-type photosensitizer, Colloid. Surface. Physicochem. Eng. Aspect. 442 (2014) 42–49.
[7] X. Zhang, S. Rehm, M.M. Safont-Sempere, F. Würthner, Vesicular perylene dye nanocapsules as supramolecular fluorescent pH sensor systems, Nat. Chem. 1 (2009) 623.
[8] J.L. Chávez, J.L. Wong, R.S. Duran, Core−Shell Nanoparticles: characterization and study of their use for the encapsulation of hydrophobic fluorescent dyes, Langmuir 24 (5) (2008) 2064–2071.
[9] A.B. Solovieva, N.S. Melik-Nubarov, T.M. Zhiyentayev, P.I. Tolstih, Kuleshov II, N.A. Aksenova, et al., Development of novel formulations for photodynamic therapy on the basis of amphiphilic polymers and porphyrin photosensitizers. Pluronic influence on photocatalytic activity of porphyrins, Laser Phys. 19 (4) (2009) 817–824.
[10] I. Moreno-Villoslada, T. Murakami, H. Nishide, Comment on "J-and H-aggregates of 5, 10, 15, 20-tetrakis-(4− sulfonatophenyl)-porphyrin and interconversion in PEG-b-P4VP micelles", Biomacromolecules 10 (12) (2009) 3341–3342.
[11] C. Toncelli, J.P. Pino-Pinto, N. Sano, F. Picchioni, A.A. Broekhuis, H. Nishide, et al., Controlling the aggregation of 5, 10, 15, 20-tetrakis-(4-sulfonatophenyl)-porphyrin by the use of polycations derived from polyketones bearing charged aromatic groups, Dyes Pigments 98 (1) (2013) 51–63.
[12] J.P. Pino-Pinto, F. Oyarzun-Ampuero, S.L. Orellana, M.E. Flores, H. Nishide, I. Moreno-Villoslada, Aerogels containing 5, 10, 15, 20-tetrakis-(4-sulfonatophenyl)-porphyrin with controlled state of aggregation, Dyes Pigments 139 (2017) 193–200.

[13] M. Gómez-Tardajos, J.P. Pino-Pinto, C. Díaz-Soto, M.E. Flores, A. Gallardo, C. Elvira, et al., Confinement of 5, 10, 15, 20-tetrakis-(4-sulfonatophenyl)-porphyrin in novel poly (vinylpyrrolidone) s modified with aromatic amines, Dyes Pigments 99 (3) (2013) 759–770.
[14] C. Díaz, J. Catalán-Toledo, M.E. Flores, S.L. Orellana, H. Pesenti, J. Lisoni, et al., Dispersion of the photosensitizer 5,10,15,20-Tetrakis(4-Sulfonatophenyl)-porphyrin by the amphiphilic polymer poly(vinylpirrolidone) in highly porous solid materials designed for photodynamic therapy, J. Phys. Chem. B 121 (30) (2017) 7373–7381.
[15] E. Araya-Hermosilla, J. Catalán-Toledo, F. Muñoz-Suescun, F. Oyarzun-Ampuero, P. Raffa, L.M. Polgar, et al., Totally organic redox-active pH-sensitive nanoparticles stabilized by amphiphilic aromatic polyketones, J. Phys. Chem. B 122 (5) (2018) 1747–1755, https://doi.org/10.1021/acs.jpcb.7b11254.
[16] E. Araya-Hermosilla, S.L. Orellana, C. Toncelli, F. Picchioni, I. Moreno-Villoslada, Novel polyketones with pendant imidazolium groups as nanodispersants of hydrophobic antibiotics, J. Appl. Polym. Sci. 132 (32) (2015).
[17] R. Araya-Hermosilla, A. Broekhuis, F. Picchioni, Reversible polymer networks containing covalent and hydrogen bonding interactions, Eur. Polym. J. 50 (2014) 127–134.
[18] R. Araya-Hermosilla, G. Lima, P. Raffa, G. Fortunato, A. Pucci, M.E. Flores, et al., Intrinsic self-healing thermoset through covalent and hydrogen bonding interactions, Eur. Polym. J. 81 (2016) 186–197.
[19] A. Nineham, The chemistry of formazans and tetrazolium salts, Chem. Rev. 55 (2) (1955) 355–483.
[20] M.E. Flores, P. Garces-Jerez, D. Fernandez, G. Aros-Perez, D. Gonzalez-Cabrera, E. Alvarez, et al., Facile formation of redox-active totally organic nanoparticles in water by in situ reduction of organic precursors stabilized through aromatic-aromatic interactions by aromatic polyelectrolytes, Macromol. Rapid Commun. 37 (21) (2016) 1729–1734.
[21] I. Moreno-Villoslada, M. Soto, F. González, F. Montero-Silva, S. Hess, I. Takemura, et al., Reduction of 2, 3, 5-triphenyl-2 H-tetrazolium chloride in the presence of polyelectrolytes containing 4-styrenesulfonate moieties, J. Phys. Chem. B 112 (17) (2008) 5350–5354.
[22] I. Moreno-Villoslada, C. Torres, F. González, M. Soto, H. Nishide, Stacking of 2, 3, 5-triphenyl-2 H-tetrazolium chloride onto polyelectrolytes containing 4-styrenesulfonate groups, J. Phys. Chem. B 112 (36) (2008) 11244–11249.
[23] E. Drent, J.J. Keijsper, Polyketone polymer preparation with tetra alkyl bis phosphine ligand and hydrogen, Google Patents, 1993.
[24] W.P. Mul, H. Dirkzwager, A.A. Broekhuis, H.J. Heeres, A.J. van der Linden, A.G. Orpen, Highly active, recyclable catalyst for the manufacture of viscous, low molecular weight, CO–ethene–propene-based polyketone, base component for a new class of resins, Inorg. Chim. Acta. 327 (1) (2002) 147–159.
[25] M.C. DeRosa, R.J. Crutchley, Photosensitized singlet oxygen and its applications, Coord. Chem. Rev. 233–234 (2002) 351–371.
[26] P.B. Merkel, D.R. Kearns, Radiationless decay of singlet molecular oxygen in solution. Experimental and theoretical study of electronic-to-vibrational energy transfer, J. Am. Chem. Soc. 94 (21) (1972) 7244–7253.
[27] M.E. Flores, N. Sano, R. Araya-Hermosilla, T. Shibue, A.F. Olea, H. Nishide, et al., Self-association of 5, 10, 15, 20-tetrakis-(4-sulfonatophenyl)-porphyrin tuned by poly (decylviologen) and sulfobutylether-β-cyclodextrin, Dyes Pigments 112 (2015) 262–273.